Overview of treatment related complications in malignant pleural mesothelioma

David J. Murphy, Ritu R. Gill

Division of Thoracic Radiology, Department of Radiology, Brigham and Women's Hospital and Harvard Medical School, Boston, MA, USA

Contributions: (I) Conception and design: All authors; (II) Administration support: All authors; (III) Provision of patients: None; (IV) Collection of data: None; (V) Data analysis: None; (VI) Manuscript writing: All authors; (VII) Final approval of manuscript: All authors.

Correspondence to: David J. Murphy, MB, BCh BAO, MRCPI, FRCR, FFRRCSI. Division of Thoracic Radiology, Department of Radiology, Brigham and Women's Hospital, 75 Francis St, Boston, MA, USA. Email: dmurphy23@bwh.harvard.edu.

Abstract: Malignant pleural mesothelioma (MPM) is an aggressive malignant neoplasm of the pleura related to asbestos exposure. Despite recent advances in therapy for MPM, the prognosis remains poor, with considerable treatment associated morbidity. Radiological assessment plays a central role in the timely identification and subsequent management of treatment related complications in MPM. This review highlights common and uncommon complications associated with and encountered in the post treatment phase.

Keywords: Malignant pleural mesothelioma (MPM); complications; imaging; computed tomography (CT); magnetic resonance imaging (MRI)

Submitted Feb 17, 2017. Accepted for publication Feb 23, 2017.
doi: 10.21037/atm.2017.03.97
View this article at: http://dx.doi.org/10.21037/atm.2017.03.97

Introduction

Malignant pleural mesothelioma (MPM) is an uncommon malignant neoplasm of the pleura with a high mortality, a median overall survival of 1 year and a 5-year overall survival of less than 10% (1). Treatment-related complications further contribute to the morbidity and early identification and timely triage of the affected patients may improve survival. In this review, we briefly describe the current and novel treatment options available to patients in MPM, with a focus on treatment related complications, and the role of imaging in their diagnosis.

Pathology, clinical features and diagnosis

There are three distinct histologic subtypes of MPM, epithelioid (approximately 65% cases), sarcomatoid (15%) and mixed/biphasic (20%) (2). Epithelioid is the most common subtype, and is associated with better outcomes. Sarcomatoid subtype has been associated with worse prognosis and can mimic sarcomas in appearance and behavior (3). The early presentation in MPM can be non-specific, with chest pain, dyspnea and cough the most common presenting symptoms. The most frequent initial imaging presentation is a unilateral pleural effusion on chest radiograph (CXR). Computed tomography (CT) is the most common cross-sectional imaging modality used for diagnosis, with a typical appearance on CT of a circumferential rind of nodular pleural thickening with or without a pleural effusion, and rarely as a focal pleural mass (2). In advanced disease, mediastinal, chest wall and abdominal invasion can occur, along with malignant adenopathy and distant metastases. CT remains the mainstay of imaging evaluation, augmented by magnetic resonance imaging (MRI) and ^{18}F-fluorodeoxyglucose positron emission tomography/CT (^{18}F FDG PET/CT) in determining tumor stage and evaluating for surgical resectability (4-6). Biphasic and sarcomatoid subtypes are typically more aggressive than the epithelial subtype, and can present with osseous or distant metastases at the time of initial diagnosis. There are no distinct imaging features

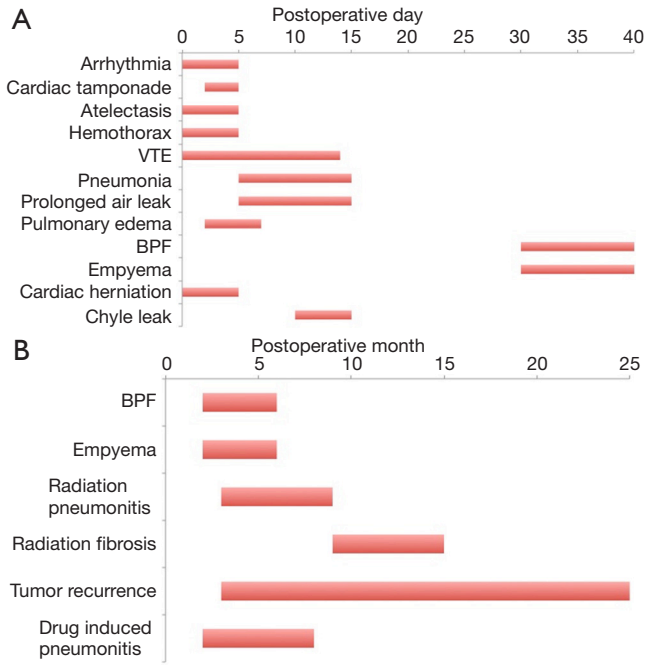

Figure 1 MPM common treatment related complications timelines. (A) Timeline of common early (days) post-operative complications for MPM cytoreductive surgery; (B) timeline of common late (months) treatment complications for MPM undergoing trimodality therapy (surgery, radiotherapy, chemotherapy). MPM, malignant pleural mesothelioma; BPF, bronchopleural fistula; VTE, venous thromboembolism.

that allow accurate differentiation of the three histologic subtypes of MPM. Promising novel quantitative MRI sequences, such as diffusion weighted imaging (DWI) have potential in differentiating epithelioid from sarcomatoid subtypes (7). Establishing a diagnosis in early stages can be problematic as pleural fluid cytology can be frequently non-diagnostic, often requiring tissue sampling via either video-assisted thoracic surgery (VATS) or CT-guided core biopsy (8).

Clinical staging is not accurate in predicting prognosis, nor can it reliably stratify patients for treatment strategies (9). Tumor volume derived from CT scans is a promising tool being evaluated as an alternate prognostic strategy to stratify patients for management algorithms (10,11). In the current clinical practice, the TNM staging system is used to assess resectability and also stage patients prior to assignment of treatment strategy. Emerging body of work on volumetric assessment will evaluate alternate strategies to stratify patients.

Treatment strategies

Treatment of MPM generally involves a multimodality approach incorporating surgery, radiotherapy and chemotherapy, with novel therapeutic modalities including heated intraoperative chemotherapy, photodynamic therapy and immunotherapy. Macroscopic complete surgical resection forms the cornerstone of management, and is the only therapeutic intervention independently associated with a survival benefit (12,13). The majority of patients with stage I–III disease with epithelial or mixed histology, and who are medically eligible, undergo trimodality treatment combining surgery, chemotherapy and radiology (14). Chemotherapy is recommended as the primary treatment in patients with unresectable or metastatic disease (14).

Surgery for MPM encompasses procedures for diagnosis and staging, debulking operations for palliation and macroscopic complete surgical resection for curative intent. Due to inter-institutional variation in surgical practice and nomenclature the International Mesothelioma Interest Group (IMIG) and International Association for the Study of Lung Cancer (IASLC) have proposed uniform definitions for the surgical techniques commonly used in MPM to allow for comparison of outcomes across centers of excellence (15). Extrapleural pneumonectomy (EPP) and extended pleurectomy/decortication (EP/D) are the most common surgical techniques performed with curative intent; the decision on which operation to perform are often based on several factors (patient-specific, surgeon-specific and institution-specific factors) (16). EP/D is associated with a lower overall perioperative mortality than EPP (30 day mortality of 1.7% *vs.* 4.5% respectively) (17,18). A meta-analysis of outcomes in patients with MPM post macroscopic complete surgical resection (EPP *vs.* EP/D) shows a higher perioperative short term mortality post EPP (4.5% *vs.* 1.7%, respectively) with no difference in long-term (2 years) survival (24% *vs.* 25% respectively) (17). The better perioperative mortality has led to a recent trend towards preference to EP/D, whenever possible (14,16,19).

Post-operative complications

Cardiac

Cardiac arrhythmias are the most common complication experienced in the after both EPP and EP/D, occurring frequently in the early postoperative period (*Figure 1*). A review of case series reporting complications in MPM

Table 1 Cumulative reported incidence of postoperative complications in case series of MPM macroscopic completer surgical resection (EPP 1,195 patients, EP/D 800 patients) (17,20-38)

Complication	EP/D (%)	EPP (%)
Arrhythmia	7.4	17.6
Pneumonia	2.0	1.6
Prolonged air leak	5.9	0.3
ARDS	0.8	4.9
Bleeding	3.9	3.2
Empyema	0.4	3.7
BPF	0.4	2.3
Chyle leak	0.8	0.4
VTE	1.4	3.3
Cardiac herniation	–	0.4
Bowel herniation	0.5	0.4
EPF	–	0.3

EPP, extra-pleural pneumonectomy; EP/D, extended pleurectomy/decortication; ARDS, acute respiratory distress syndrome; BPF, bronchopleural fistula; VTE, venous thromboembolism; EPF, esophagopleural fistula.

patients post attempted curative surgical resection (approximately 1,195 EPP and 800 EP/D patients) demonstrates a postoperative arrhythmia rate of 17.6% post EPP and 7.4% post EP/D (17,20-38) (*Table 1*). Supraventricular tachyarrhythmias, such as atrial fibrillation, are the most common, and can increase the risk of systemic embolization and cerebral and mesenteric ischemia.

Inflammatory epicarditis is a potentially serious early complication caused by epicardial inflammation post pericardial resection. It is more common after left-sided surgery, and can result in pericardial constriction, necessitating re-exploration. Echocardiography (either transthoracic or transesophageal) is the principal imaging modality used for diagnosis, depicting signs of constriction. These include abnormal ventricular septal motion (from ventricular interdependence), dilated inferior vena cava (IVC), tubular appearance of the right ventricle (RV), and diastolic flow reversal in the hepatic veins (39). Routine pericardial reconstruction has reduced the incidence of this complication (37).

Cardiac tamponade is a rare complication that can result from a significant pericardial effusion or an overly constrictive pericardial patch. It can present immediately after surgery when the patient is turned supine from the lateral intraoperative position with immediate reduction in cardiac output, or may occur on day 2–4, presenting more insidiously with diminished urine output. Echocardiography is the initial imaging modality of choice, with diagnostic features including diastolic cardiac chamber compression, most notably of the right atrium (RA) and RV in the presence of a pericardial effusion, paradoxical motion of the interventricular septum and compression of the IVC (40). Although echocardiography is the imaging modality of choice in cases of suspected tamponade, these patients may need to undergo a CT scan to exclude other postoperative complications, such as pulmonary embolus. The major features of cardiac tamponade on CT scan include enlargement of the superior vena cava (SVC), enlargement of the IVC, periportal edema (manifesting as periportal linear low attenuation), reflux of contrast into the IVC and hepatic veins, reflux of contrast into the azygos vein, enlargement of the hepatic and renal veins and flattening of the RV free wall occurring in the context of a pericardial effusion (40,41). These imaging features are not specific for tamponade; therefore, it is vital for the radiologist to have a high index of suspicion in symptomatic patients post pericardial reconstruction.

Cardiac herniation and torsion are rare complications that can occur following pericardial resection and reconstruction, and are more common post EPP, with a reported incidence of approximately 0.4% (*Table 1*) (17,20-38). Herniation of a cardiac chamber through the pericardial patch usually occurs in the early postoperative period, and can be triggered in a vulnerable patient by a sudden change in position or the application of negative pressure to a chest tube. When the heart herniates to the right, signs and symptoms occur secondary to compression of the SVC by resultant cardiac torsion. Leftward herniation causes hypotension and tachycardia due to ventricular strangulation by the pericardial patch (37,42). Diagnosis is often made on clinical grounds, with patients needing urgent operative management. Herniation to the left manifests on CXR as a sharp bulge in the left cardiac contour created by the protruding cardiac chamber, so-called "collar sign", with the cardiac apex remaining in the left hemithorax (43). In right-sided herniation, the cardiac apex is displaced into the right hemithorax, causing narrowing and obstruction of the SVC at the cavoatrial junction (*Figure 2*). The "snow cone" sign is an early CXR sign of right cardiac herniation manifesting as a hemispheric bulging appearance of the right heart border

Figure 2 CXR (A) and CT with IV contrast (B) in a 22-year-old patient demonstrate a large soft tissue tumor (star) in the right hemithorax causing deviation of the heart and mediastinum into the left hemithorax. The patient underwent a right pneumonectomy, and became hypotensive immediately post-op: a portable CXR (C) demonstrates absence of the cardiac silhouette in the left hemithorax, and a pulmonary arterial catheter (arrow) with an abnormal rightward orientation (curved arrow); these features are consistent with cardiac herniation and volvulus. The patient was undergoing immediate exploratory thoracotomy, but unfortunately expired. CXR, chest radiograph; CT, computed tomography.

into the pneumonectomy space, caused by partial cardiac herniation (44).

Pulmonary

Atelectasis refers to pulmonary parenchymal collapse, usually secondary to retained secretions or aspiration causing mucus plugging. It is an early post-operative complication, occurring more commonly post EP/D on the operated lung, and can occur in the contralateral lung (*Figure 1*). The radiographic appearances depend on the extent of lung affected. Subsegmental atelectasis usually appears as a thin, linear band like opacity on CXR/CT, usually most marked in the lower lobes. Secondary signs include displacement of the fissures due to volume loss, bronchovascular crowding, and pulmonary parenchymal enhancement on CT with IV contrast. Lobar atelectasis/collapse is a potentially serious complication, especially in patients post EPP; these patients are managed with frequent bronchoscopy to clear secretions and prevent collapse in the remaining lung. Lobar collapse varies in CXR appearance depending on the lobe involved. Right upper lobe collapse appears as increased density in the right upper and mid-zones with elevation of the right horizontal fissure and hilum. Left upper lobe collapse manifests as a veil-like opacity in the left upper zone with elevation of the left hemidiaphragm, with or without a crescentic lucency adjacent to the aortic arch resulting from hyperexpansion of the superior segment of the left lower lobe (luftsichel sign). Right middle lobe collapse causes ill definition of the right heart border on the frontal radiograph, appearing as a triangular anterior density on the lateral radiograph. Lower lobe collapse manifests as medial triangular opacification with elevation of the ipsilateral hemidiaphragm, with loss of the lateral descending aorta border in left lower lobe collapse. Therefore, a high degree of vigilance and careful scrutiny of the postoperative radiographs can help reduce perioperative morbidity and mortality.

Hemothorax is caused by bleeding into the thoracic cavity, and typically occurs in the early post-operative period (hours to days) (*Figure 1*). Significant bleeding is more common in patients post EP/D rather than EPP, with an approximate incidence of 3.9% *vs.* 3.2% respectively (*Table 1*) (17,20-38). Stripping the visceral pleura during EP/D from the lung surface exposes a raw surface that can bleed easily. Other potential causes include intercostal vessel injury and ligature slippage from a major vessel. Delayed hemorrhage may occur secondary to consumptive coagulopathy lysing fibrin plugs in the dissection field; this can be a potentially serious complication as mesothelioma patients are often in a hypercoagulable state (45). Hemothorax typically results in rapid opacification of the postoperative hemithorax, manifesting as pleural fluid on CXR. CT can distinguish between simple and hemorrhagic fluid, which appears heterogeneously high attenuation on

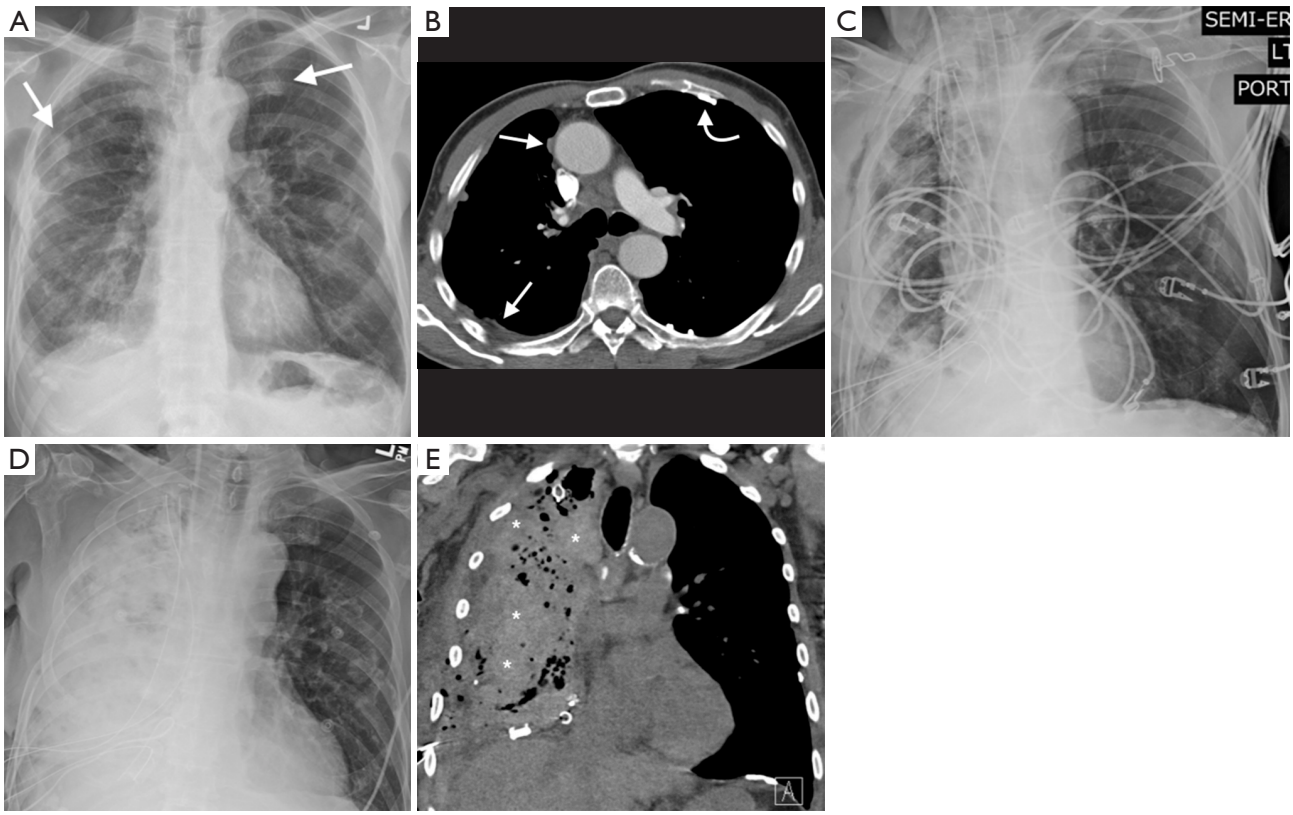

Figure 3 A 78-year-old man with right epithelioid mesothelioma. Initial CXR (A) demonstrates a right pleural effusion with bilateral calcified pleural plaques (arrows). Axial image from a post-contrast CT thorax (B) demonstrates volume loss in the right hemithorax with calcified pleural plaques (curved arrows) and right nodular pleural thickening (arrows); biopsy confirmed right epithelioid mesothelioma. The patient underwent right extended pleurectomy/decortication with diaphragmatic resection and reconstruction. CXR day 1 post-surgery (C) demonstrates subcutaneous emphysema in the right chest wall with 3 chest drains in situ. On day 4 post-surgery the patient's hematocrit dropped, and a CXR (D) demonstrated new, extensive opacification of the right hemithorax. Coronal image from a same-day non-contrast CT thorax (E) demonstrates extensive high attenuation material in the right hemithorax (stars) consistent with pulmonary hemorrhage. The patient underwent exploration with identification of a bleed from an intercostal vein, which was successfully ligated. CXR, chest radiograph; CT, Computed tomography.

non-contrast CT with internal fluid-fluid levels (*Figure 3*). Multiphase CT angiography with a non-contrast, bolus tracked arterial phase and delayed phase (approximately 70 s) can be useful in identifying the source of intrathoracic arterial hemorrhage, such as an injured intercostal vessel.

Pulmonary edema typically occurs after 2–3 days, and is more frequent post EPP, especially on the right (*Figure 1*) (16). This is thought to be caused by increased pulmonary blood flow to the left lung which overwhelms the lymphatics that usually receive approximately 45% of pulmonary blood flow (46). The edema tends to involve the lower lobe initially due to differential differences in blood flow between the upper and lower lobes, often mistaken as pneumonia or aspiration. Other risk factors include excessive perioperative fluids, blood and blood products transfusion. Pulmonary edema manifests on CXR as peribronchovascular cuffing, Kerley lines, pulmonary effusions, and diffuse air space opacities in severe cases of alveolar edema. Patchy ground glass opacities and smooth septal thickening with bilateral pleural effusions constitute the typical CT appearances. Severe pulmonary edema may be indistinguishable on imaging from acute respiratory distress syndrome (ARDS) (47).

Pneumonia post-EPP is one of the leading causes of death (37), occurring in approximately 2% patients after both EPP and EP/D (*Table 1*) (17,20-38). Common

causes of infection include aspiration of gastric contents, bacterial colonization of atelectatic lung and presence of a bronchopleural fistula (BPF). The most common radiographic appearance is multifocal patchy consolidation in a bronchocentric distribution, representing a bronchopneumonia, lobar consolidation is less frequent (43,46). CT demonstrates consolidation and ground glass opacification (GGO), with mucus plugging and bronchial wall thickening suggestive of aspiration as an etiology. Lack of enhancement of opacified lung on contrast-enhanced CT is a useful feature to distinguish atelectasis from pneumonia. Patients with prolonged infection or those with large volume aspiration are at risk for necrotizing pneumonia and/or lung abscess formation, characterized by gas or air-fluid levels within the consolidation.

Venous thromboembolism (VTE), comprising of deep venous thrombosis (DVT) and pulmonary embolus (PE) are uncommon, but potentially serious post-operative complications, with a cumulative reported incidence of 3.3% post EPP and 1.4% post EP/D (*Table 1*) (17,20-38). The combination of chemotherapy and baseline hypercoagulable state increases the perioperative VTE risk. PE was identified by Sugarbaker *et al*. as the most common cause of mortality in patients post EPP (37). Doppler ultrasonography is the investigation of choice in patients with suspected DVT. CT pulmonary angiography (CTPA) is the imaging test of choice in suspected acute PE, manifesting as a central occlusive pulmonary arterial filling defect. If negative for PE, CT is useful in identifying alternate potential causes of hypoxia, such as pulmonary edema or pneumonia. Prophylactic therapeutic anticoagulation and early postoperative mobilization may help reduce the risk of VTE in MPM patients undergoing major cytoreductive surgery (48).

ARDS is more common in patients post EPP than EP/D, with a cumulative reported incidence of 4.9% *vs.* 0.8% respectively (*Table 1*) (17,20-38). It has a high mortality, especially in the EPP group, with a mortality of >80% (17). ARDS is a clinic-radiological diagnosis of acute respiratory failure resulting in profound hypoxia with widespread opacification that cannot be attributed to volume overload or cardiac failure, occurring within a week of a defined trigger, as defined by the Berlin definition (49). The etiology is often multifactorial, including diffuse endothelial damage, blood transfusion, lymphatic damage, aspiration, pneumonia and empyema. The consequent diffuse alveolar damage increases alveolar permeability, evolving over weeks through exudative, inflammatory and fibroproliferative phases (50). The CXR appearances can be difficult to distinguish from cardiogenic pulmonary edema, demonstrating extensive airspace opacification. The CT appearances are varied, with areas of GGO and consolidation interspersed with normal lung. The normal lung tends to be anterior, with the consolidative opacities typically in the dependent portions of the lung, with the areas of GGO lying between the two (50). There is often an apicobasal gradient of pulmonary opacification (*Figures 4*,*5*). In contradistinction to cardiogenic edema, the vascular pedicle is normal and septal lines and pleural effusions are not typical. The principal treatment for ARDS is mechanical ventilation, and these patients are prone to barotrauma causing pneumothoraces, pneumomediastinum and interstitial emphysema. If the patient survives the initial course, a fibroproliferative phase can ensue caused by fibroblast proliferation, resulting in fibrosis and traction bronchiectasis, most marked in the anterior portions of the lungs (50).

Prolonged air leak arising from the lung parenchyma is a common complication in EP/D patients, occurring in approximately 6% of cases; unsurprisingly it is rare post EPP (0.3%) (*Table 1*) (17,20-38). It results from persistent air leak from open bronchoalveolar spaces, usually damaged during resection of the visceral pleura, and manifests on imaging as persistent pneumothorax, pneumomediastinum and subcutaneous emphysema. If an air leak persists for more than 5–7 days it can be problematic, increasing hospital stay and risk of infection (*Figure 6*). They are managed by maintaining chest tubes on mild suction, graduating to water seals and using pneumostat when needed (45).

BPF occur when there is an open connection between the bronchial tree and the thoracic cavity. Acute BPF usually occur within the first two weeks, and is more common after EPP than EP/D (2.3% *vs.* 0.4% respectively, *Table 1*) (17,20-38). BPFs are more common following right EPP, probably due to the wider bronchial stump and single bronchial arterial supply (43,46). Risk factors include prolonged mechanical ventilation, preoperative radiation treatment, fever, infection and excessive mucus pooling in the bronchial stump (16). BPFs are more common as a late postoperative complication (weeks to months, *Figure 1*), occurring in immunocompromised patients most commonly due to infection or recurrent tumor at the bronchial stump. Surgical treatment is often required, similar to that required in empyema (outlined below). The major radiographic appearances of BPF are failure of the post-

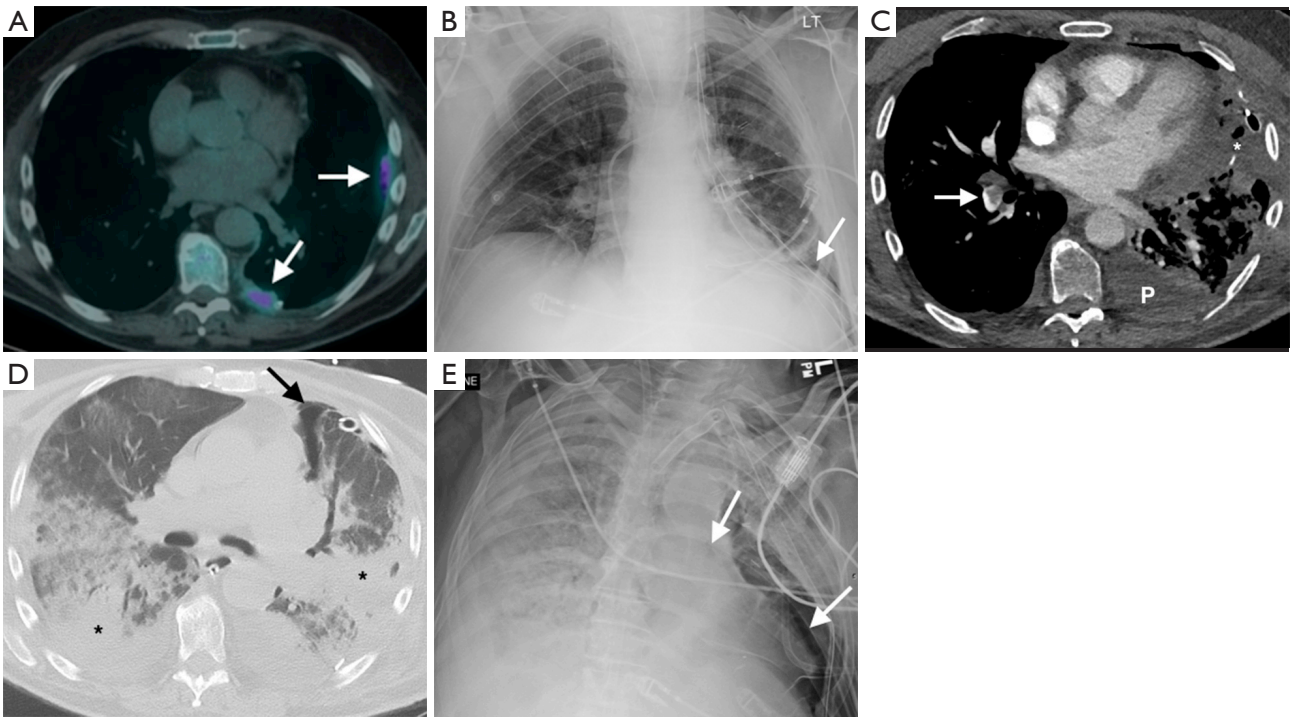

Figure 4 A 68-year-old man with left epithelioid mesothelioma. Axial 18F-FG PET/CT image (A) demonstrated FDG avid left nodular pleural thickening (arrows). A left extended pleurectomy/decortication with pericardial and diaphragmatic reconstruction was performed. Immediate post-operative CXR (B) demonstrates a small left pneumothorax, with the linear lucent appearance of the diaphragmatic reconstruction (arrow). The patient developed hypoxia on post-op day 10; axial image from a CT pulmonary angiogram (C) demonstrates a pulmonary embolus in the right lower lobe pulmonary artery (arrow), with a left pleural effusion (P) and consolidation in the lingula (star) concerning for pneumonia. The patient was anticoagulated and treated with antibiotics, but continued to deteriorate. Axial image from a non-contrast CT thorax on post-op day 17 (D) demonstrates diffuse bilateral ground glass opacities with dependent consolidation (stars) and a persistent left pneumothorax (arrow); the overall clinical and radiological picture was concerning for ARDS, and the patient was subsequently placed on ECMO. CXR on post-op day 35 (E) demonstrates almost complete opacification of the right lung, with extensive airspace opacities in the left lung, pneumopericardium (arrows) and ECMO catheter in the SVC. 18F FDG PET/CT,18F-fluorodeoxyglucose positron emission tomography/Computed tomography; FDG, fluorodeoxyglucose; CXR, chest radiograph; ARDS, acute respiratory distress syndrome; ECMO, extra-corporeal membrane oxygenation; SVC, superior vena cava.

pneumonectomy space to fill with fluid, a drop in the air-fluid level in the postoperative thorax. The re-appearance of air in a previously completely opacified hemithorax. CT demonstrates an air-fluid level in the thorax, and the source of BPF can occasionally be seen on CT, with minimum intensity projection (MinIP) useful in sourcing the location of BPF. Nuclear medicine studies utilizing ventilation study with radioactive inhaled gases may be needed to identify very small or pinhole sized BPF.

Empyema, also known as pyothorax, is infected fluid in the thoracic cavity. It is more common after EPP (3.7%) than EP/D (0.4%), with a high morbidity (17,20-38). Symptoms are often indolent, requiring a high index of suspicion for diagnosis. Early empyema (first 30 days) is usually due to residual pleural infection or intraoperative contamination. This can be prevented by high volume lavage of the pneumonectomy cavity and prophylactic perioperative antibiotics (37,45). Rapid fluid filling of the post pneumonectomy space is the most common radiographic manifestation of empyema in the early post-operative period. CT with contrast demonstrates pleural fluid with surrounding soft tissue enhancement. Late empyema (greater than 30 days) is often associated with a BPF, which can be identified on CT. Empyema is often treated by removal of the pericardial and diaphragmatic patches and creation of a Clagett window; this involves

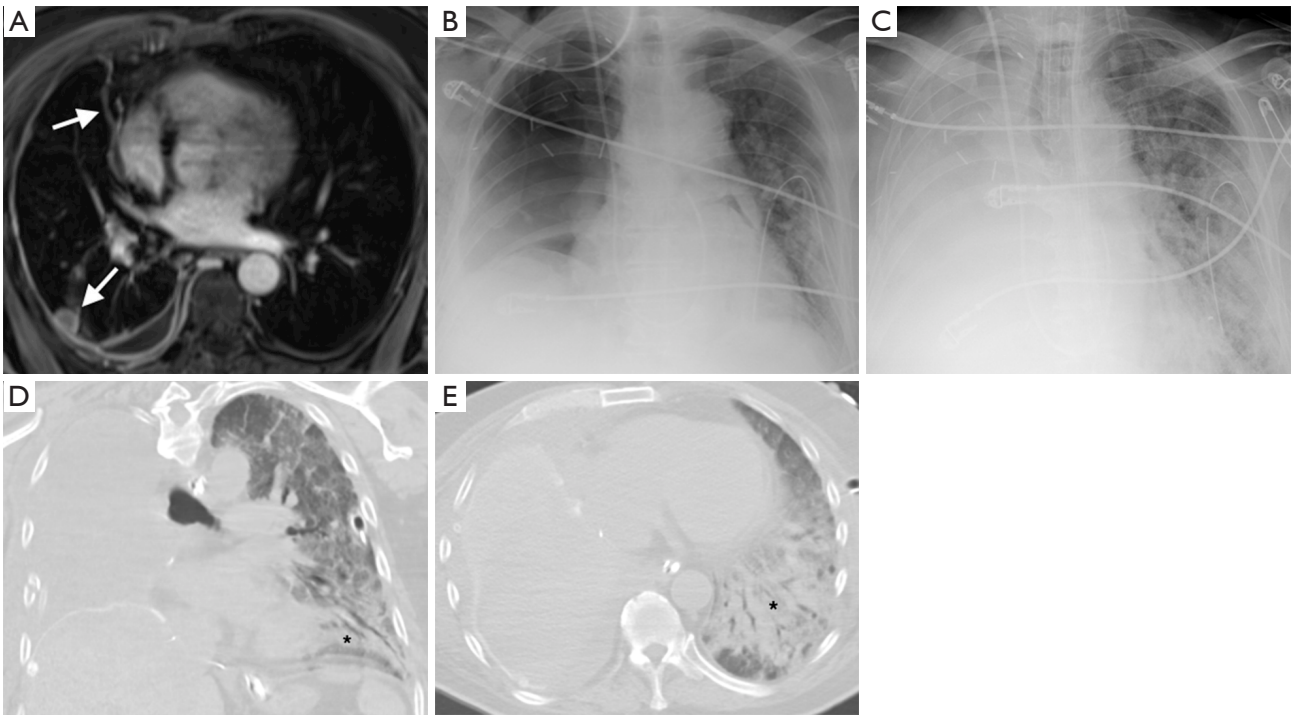

Figure 5 A 72-year-old man with a right epithelioid mesothelioma. Axial image (A) from a T1 weighted fat suppressed post gadolinium sequence from preoperative MRI demonstrates enhancing nodular right pleural thickening (arrows) with a small pleural effusion. Day 1 post-op CXR (B) demonstrates a gas filled right hemithorax post right EPP with pericardial and diaphragmatic reconstruction. The patient developed hypoxia post-surgery, with a CXR on postop day 7 (C) demonstrating worsening air space opacities in the left mid and lower zone, concerning for pulmonary edema or pneumonia. Note the progressive fluid filling of the right pneumonectomy space. Coronal (D) and axial (E) images from a non-contrast CT thorax on day 12 post-surgery demonstrate diffuse ground glass opacities throughout the left lung with left lower lobe consolidation with bronchial dilatation (star) concerning for ARDS. MRI, magnetic resonance imaging; CXR, chest radiograph; EPP, extrapleural pneumonectomy; CT, Computed tomography.

forming an open window in the lateral chest wall, allowing irrigation and free drainage of the thoracic cavity (*Figures 7,8*) (45). This window is then closed when the infection has resolved. If present, an underlying BPF needs to be repaired in order to prevent re-infection. Early empyema without a BPF may occasionally be managed by closed thoracoscopic debridement and pulsed irrigation in an effort to preserve the pericardial and diaphragmatic patches. BPF may be managed with surgical repair or with placement of a covered bronchial stent. CT curved multiplanar reformats (MPRs) are useful in identifying the source of a BPF and in planning bronchial stent placement (*Figure 8*). These curved MPRs provide an anatomical assessment of the bronchial defect, allowing for accurate stent sizing. Three-dimensional (3D) segmented volume rendered (VR) reformats can be helpful in planning these often-complex procedures.

Mediastinal shift is a potentially fatal early complication post EPP. EPP is associated with greater postoperative fluid shifts than standard pneumonectomy due to rapid filling of the pneumonectomy space along with the pericardial and/or diaphragmatic reconstruction. This may result in excessive mediastinal shift away from the pneumonectomy space into the contralateral thorax, causing retained secretions, atelectasis and respiratory compromise. Postpneumonectomy syndrome is a late complication of EPP, usually manifesting as progressive dyspnea months to years after surgery. It is classically described post right pneumonectomy, and is caused by shift of the mediastinum into the pneumonectomy space resulting in tracheobronchial compression (51). CT is the imaging modality of choice, demonstrating ipsilateral mediastinal shift with narrowing of the trachea and left main bronchus caused by compression between the pulmonary artery anteriorly and the thoracic vertebrae/aorta posteriorly.

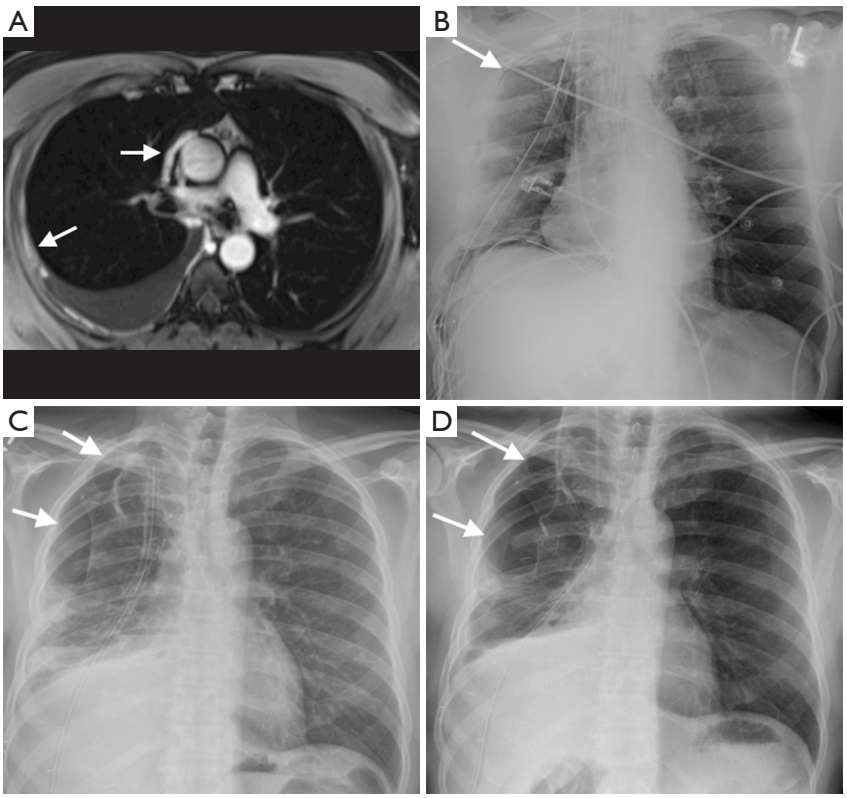

Figure 6 A 59-year-old man with right epithelioid mesothelioma. Axial T1 weighted fat saturated post gadolinium (A) from a preoperative MRI demonstrates multifocal, circumferential enhancing right pleural nodularity (arrows), with a small right pleural effusion. The patent underwent a right EP/D with diaphragmatic and pericardial reconstruction and multiple lung wedge resections. Day 1 post-operative CXR (B) demonstrates a small right pneumothorax (arrow) with three right-sided chest drains. CXR one-month post-op (C) demonstrates a persistent loculated right pneumothorax (arrows) consistent with a persistent air leak. The right pneumothorax persists on CXR 7 week post-surgery (arrows, D). MRI, magnetic resonance imaging; EP/D, extend pleurectomy/decortication; CXR, chest radiograph.

It can occur post left EPP, but is less common. The current practice of controlled filling of the pneumonectomy space with a manometer attached to a Robnell catheter helps prevent excessive mediastinal shift (37,52).

Other complications

Chylothorax

Injury to the thoracic duct or one of the main lymphatic channels can cause leakage of lymph into the thoracic cavity, causing a chylothorax. It typically develops 10 days post-surgery, manifesting on CXR as rapid filling of the resection space causing contralateral mediastinal shift. CT can occasionally distinguish chyli from simple pleural fluid, especially after a fatty meal when the chyle is of low (fat) attenuation. Diagnosis can be confirmed by checking the fluid triglyceride level, which is usually elevated (53). Interventional radiology guided thoracic duct embolization is often the initial treatment of choice; this involves catheterization of the cisterna chyli, performing a lymphangiogram to identify the source of leak and embolization of the thoracic duct proximal to the site of leak (*Figure 9*) (54). Non-contract MRI is useful prior to this procedure, helps in localization of the cisterna chyli and thoracic duct, facilitating percutaneous access (54). The cisterna chyli is best identified on heavily T2 weighted imaging (T2 weighted single shot fast spin echo sequences) as a high signal oval structure lying between the aorta and IVC in the upper lumbar/retrocrural region (55). MRI is not useful in identifying the source of the chyle leak; the test of choice continues to be a lymphangiogram.

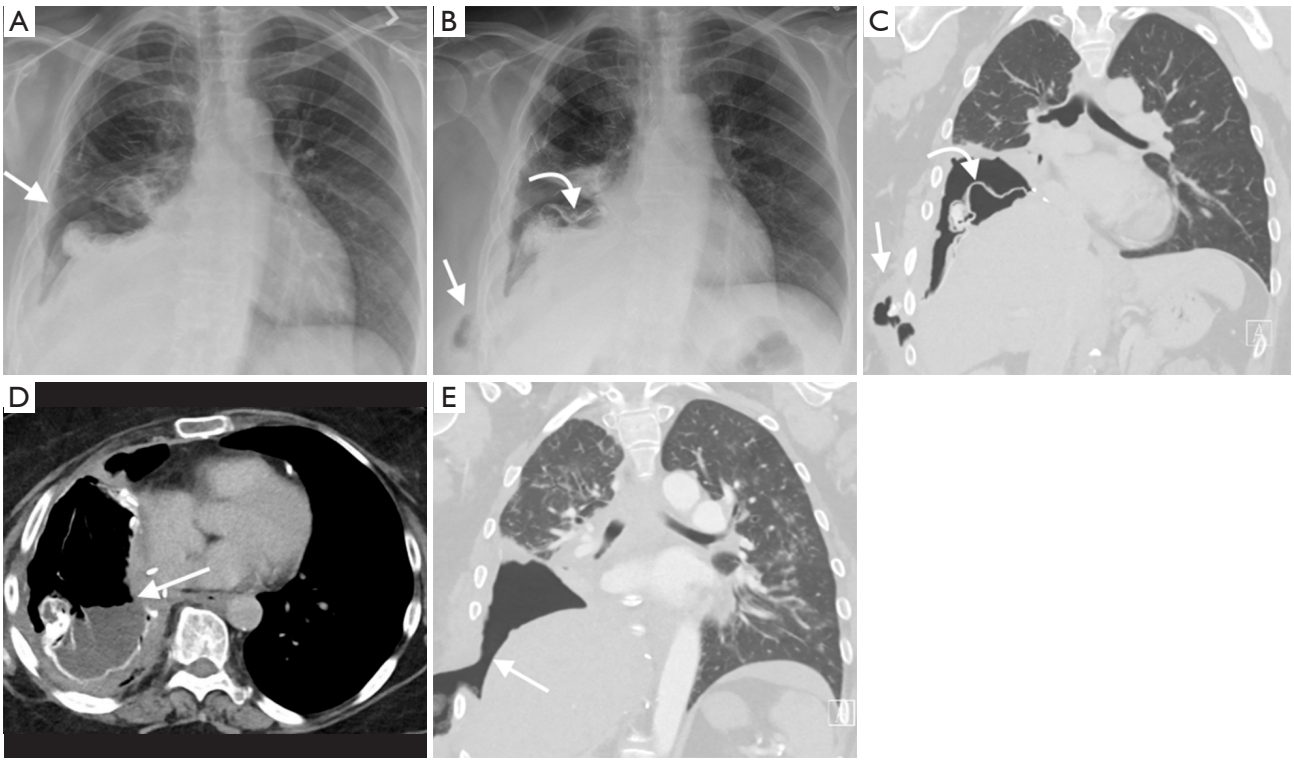

Figure 7 A 65-year-old woman with right epithelioid mesothelioma underwent a right EP/D with diaphragmatic reconstruction. CXR 2-year post-op (A) demonstrates a persistent loculated right basal hydropneumothorax (arrow). The patient subsequently presented two and a half years post-surgery with fever and purulent chest wall discharge. CXR (B) demonstrates new subcutaneous gas in the right chest wall (arrow) and new gas under the right diaphragmatic reconstruction (curved arrow), concerning for empyema formation. Coronal image from a CT thorax (C) demonstrates a right lateral chest wall gas and fluid collection (arrow) and air under the diaphragmatic reconstruction (curved arrow). Axial image from a CT thorax (D) demonstrates a collection under the right diaphragmatic reconstruction with an air-fluid level (arrow), concerning for empyema. The diaphragmatic flap was removed, the empyema evacuated and a right Clagett window formed, as demonstrated on this coronal image from a post-contrast CT thorax (arrow, E). A small bronchopleural fistula was found during the operation, and the drained fluid grew *Aspergillus sp*. EP/D, extend pleurectomy/decortication; CXR, chest radiograph; CT, Computed tomography.

Diaphragmatic graft defect

The diaphragmatic patch is usually made of gore tex, and will appear initially as a radiolucent linear structure on CXR, becoming radiopaque over a number of days (43). A defect in the patch can manifest as herniation of abdominal viscera into the thoracic cavity with incarceration and strangulation of the bowel, and can result in ischemia and perforation. Diaphragmatic patch rupture causing gastrointestinal herniation has an approximate equal incidence post EPP and EP/D of 0.5% (*Table 1*) (17,20-38). The presence of complex gas patterns in the postoperative thorax on CXR is suggestive of bowel herniation, with CT providing definitive diagnosis (45). The gore tex patch is a linear high density structure on CT in the expected position of the diaphragm; discontinuity or foreshortening of this represents graft rupture, with the presence of abdominal viscera within the thoracic cavity signifying herniation (43). Urgent laparotomy may be required to reduce the herniated abdominal viscera and repair the defect.

Esophagopleural fistula (EPF)

This is a rare (<1%) complication described in EPP patients with a high mortality (17,20-38). It usually manifest months after surgery, although it may occur in the early postoperative period secondary to intraoperative esophageal injury. Precipitating factors include local

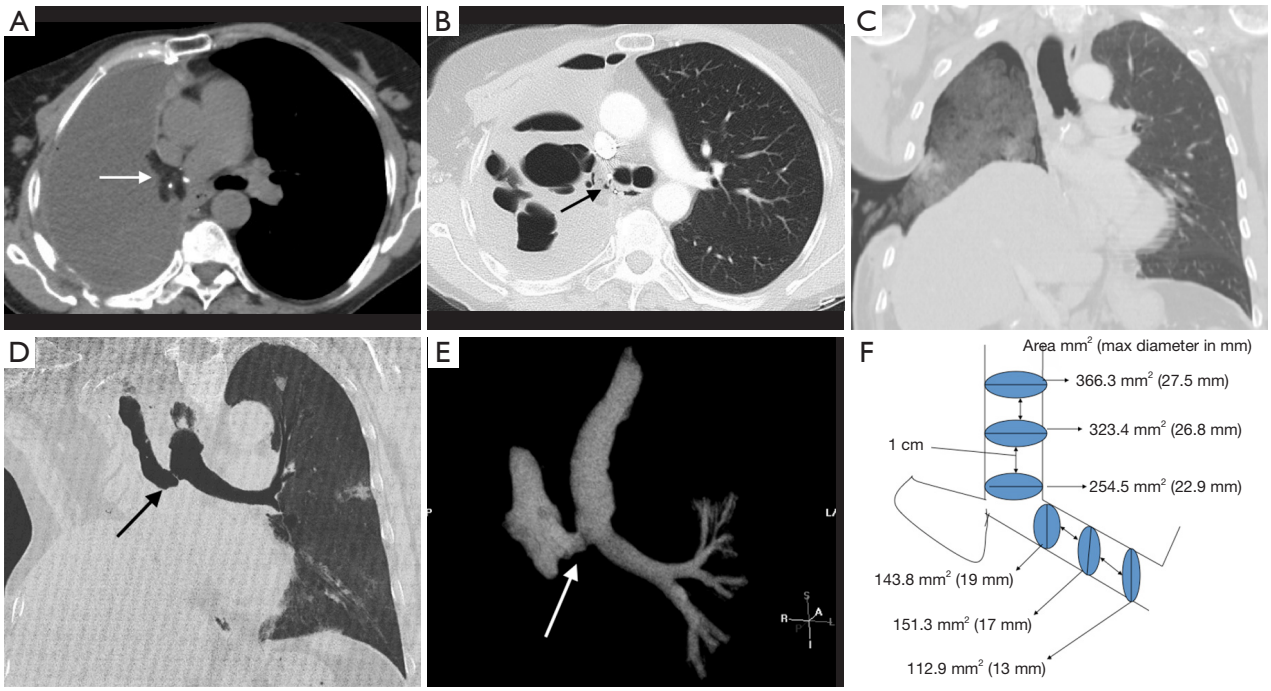

Figure 8 A 75-year-old woman with epithelioid mesothelioma underwent right EPP. Postoperative CT thorax (A) demonstrates a fluid filled right hemithorax with an omental flap buttressing the right bronchial stump (arrow). Two months later, she presented with fevers and rigors: CT thorax (B) demonstrates multiple pockets of gas in the previously fluid filled right hemithorax consistent with an empyema. Pockets of gas adjacent to the right bronchial stump represent the site of a BPF (arrow). This was treated with surgical repair and formation of a right Clagett window (C). Following closure of the right thoracostomy, the patient represented with fever a number of months later. Coronal CT thorax MinIP (D) demonstrates a new gas collection in the right hemithorax, communicating with the right bronchial stump consistent with a recurrent BPF (arrow). Bronchial stent placement was performed to close the defect, which can be planned from the CT data. Segmented volume rendered image of the tracheobronchial tree (E) provides a 3D assessment of airway anatomy. Schematic (F) demonstrates sites of area measurement of the tracheobronchial tree, useful in bronchial stent sizing. EPP, extrapleural pneumonectomy; BPF, bronchopleural fistula; MinIP, minimum intensity projection; CT, computed tomography.

tumor recurrence, malignant adenopathy, radiation and infection (56). EPF usually present with an empyema with the presence of ingested air and food particles in the empyema cavity. Fluoroscopy or CT with water soluble oral contrast may directly demonstrate the fistula; placing the patient's pneumonectomy side down during oral contrast administration can aid delineation of the fistulous tract (46,57). Surgical treatment is usually required to repair the esophageal wall to prevent continued infection of the pneumonectomy space.

Radiotherapy

Radiation treatment is used in conjunction with surgery and chemotherapy in patients with non-metastatic MPM with an associated survival benefit (58). Radiotherapy is recommended by the National Cancer Control Network (NCCN) for patients with resectable MPM post-surgery to improve local control (14). Modern radiotherapy techniques, such as the use of intensity-modulated radiotherapy (IMRT), allows limitation of the high dose area tightly to the target area, sparing radiation exposure of adjacent organs (59). Although usually administered as an adjuvant therapy post-surgery, recently radiation has been proposed as a neo-adjuvant treatment ("SMART" approach) prior to EPP in patients with resectable disease without a significant increase in perioperative mortality (60,61). The major complication of radiotherapy for MPM is the development of radiation induced lung disease, a potentially fatal complication, especially post EPP (62).

There are two distinct phases of radiation induced lung disease, with different imaging appearances. Radiation

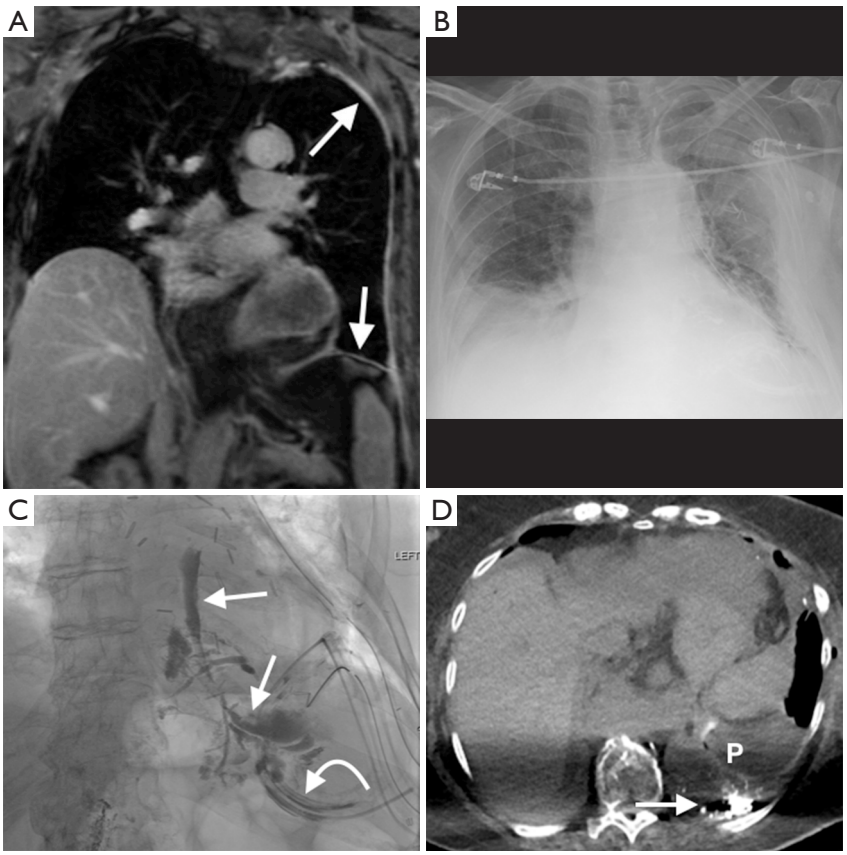

Figure 9 A 77-year-old woman with a left epithelioid mesothelioma underwent a left EP/D with diaphragmatic reconstruction. Coronal image from pre-operative fat-suppressed T1 weighted post-gadolinium sequence (A) demonstrates enhancing left circumferential nodular pleural thickening (arrow). In the early post-operative period, there was high fluid output from left pleural drain with a high triglyceride content, concerning for a chyle leak. A CXR on post-op day 10 (B) demonstrates a left hydropneumothorax with a left chest tube in situ. Frontal spot radiograph from a subsequent lymphangiogram (C) post inguinal lymph node 15ml lipiodol injection demonstrates layering extravasation into the left hemithorax (arrows) consistent with a chyle leak. Note lymphangiographic contrast material draining via the left inferior chest drain (curved arrow). Axial image from a non-contrast CT thorax (D) demonstrates loculated left pleural effusion (P), with retained lymphangiographic contrast (arrow) in the left hemithorax. Attempted interventional radiology thoracic duct embolization was unsuccessful, and the patient subsequently underwent surgical thoracic duct ligation. EP/D, extended pleurectomy/decortication; CXR, chest radiograph; CT, Computed tomography.

pneumonitis usually occurs 1–6 months after completion of treatment, with a later phase of chronic radiation fibrosis occurring 6–12 months after therapy ends (63). The extent of lung injury usually corresponds to the margins of the irradiated field. Radiation pneumonitis manifests on CT as ground glass opacities and consolidation within the distribution of the radiation field, with occasional development of a pleural effusion; radiation fibrosis on CT appears as a well-defined area of volume loss with architectural distortion and traction bronchiectasis (*Figure 10*) (63). Patients with radiation pneumonitis are often treated with steroids, as this can prevent development of subsequent fibrosis (64). Although the use of IMRT does limit the development of radiation induced lung disease in the remaining lung post EPP, this risk is not completely eliminated (59). IMRT is used successfully for local control in patients undergoing lung-sparing cytoreductive surgery, with recent data suggesting an approximate 30% risk of developing radiation pneumonitis in the treated hemithorax with the use of IMRT post EP/D (65).

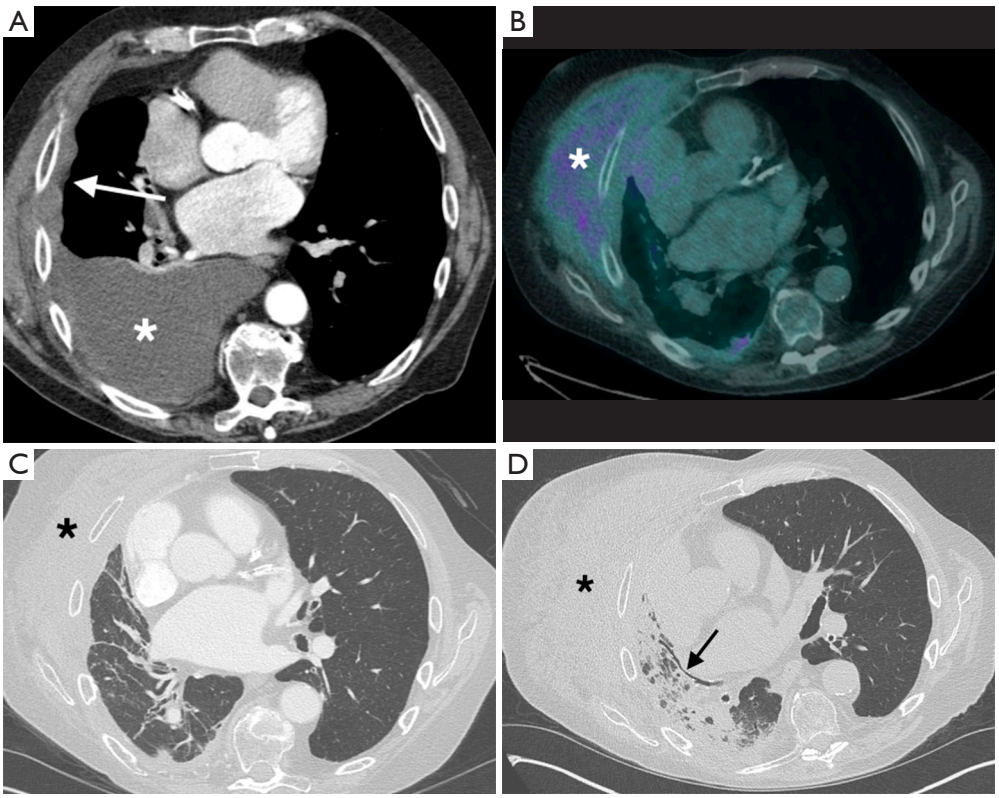

Figure 10 A 77-year-old man with right epithelioid mesothelioma underwent EP/D. Pre-operative CT thorax with IV contrast (A) demonstrates a large right pleural effusion with nodular pleural thickening in the right hemithorax (arrow). Follow-up ^{18}F-FDG PET/CT 1-year post right EP/D (B) demonstrates a large FDG-avid soft tissue mass in the right anterolateral chest wall (star) consistent with local tumor recurrence. This was subsequently treated with radiotherapy. CT thorax during the radiation treatment (C) shows reduction in size of the chest wall mass (star) with linear atelectasis in the right lung. 3 months after completion of radiation treatment, the patient developed progressive dyspnea and underwent a CT thorax (D), which demonstrates new consolidative and ground glass opacities in the right lung in a predominantly peribronchial distribution with bronchial dilatation (arrow). These imaging appearances are consistent with radiation pneumonitis. EP/D, extended pleurectomy/decortication; ^{18}F-FDG PET/CT, ^{18}F-fluorodeoxyglucose positron emission tomography/Computed tomography; FDG, fluorodeoxyglucose.

Systemic therapy

Chemotherapy is an integral component of the trimodality treatment of MPM. Combination chemotherapy is superior to monotherapy, with higher response rates to platinum-based regimens (1); the NCCN recommends cisplatin/pemetrexed regimen as first line agents (14). Cisplatin is a platinum based agent that causes cell death by binding to DNA causing crosslinking; it is associated with cardiac arrhythmias, hypersensitivity reactions, with case reports of cisplatin-induced eosinophilic pneumonia (66). Pemetrexed is a very active cytotoxic agent that acts by impairing folate metabolism. It is associated with a number of pulmonary toxicities, including drug-induced pneumonitis (67,68), diffuse alveolar hemorrhage (69), exacerbation of underlying interstitial lung disease (70) and ARDS (71). Gemcitabine is used in patients who cannot tolerate pemetrexed; this is a nucleoside analog agent with potential for pulmonary toxicity, such as pneumonitis, eosinophilic pneumonia, pulmonary fibrosis and diffuse alveolar damage (72).

Intracavitary chemotherapy has been used to help local delivery to surgical margins with less toxicity than systemic therapy. Heated intraoperative chemotherapy (HIOC) is postulated to increase local drug absorption and cytotoxicity, with a reported survival benefit in patients with epithelioid MPM (73). Cisplatin is the most common agent used, with renal toxicity a potential complication (19). The use of renal chemoprotective agents such as amifostine

and sodium thiosulphate may reduce cisplatin-associated nephrotoxicity (74).

Intracavitary photodynamic therapy (PDT) is another potential localized therapy employed in patients undergoing surgery. PDT is a light based treatment consisting of the localized administration of a photosensitizing agent causing release of oxygen free radicals resulting in cell death when exposed to a specific wavelength of light, with potential additional immunological benefit (31). Friedberg *et al*. incorporate PDT at the time of EP/D into the multimodality treatment of MPM with promising initial results; this cohort demonstrated a high rate of postoperative pneumonia (21%), possibly attributable to intraoperative PDT (75).

Advances in genomic medicine have led to the advent of numerous effective targeted therapies in lung cancer (76). This approach is being applied to MPM systemic therapy, with a number of more targeted agents being used, such as bevacizumab, a monoclonal antibody against vascular endothelial growth factor (VEGF) (1,14). Anti-VEGF agents have been used extensively in other malignancies, especially in non-small cell lung cancer, where there is an increased risk of pulmonary hemorrhage, tumor necrosis and cavitation (77). One of the most active areas of research in mesothelioma research is in the use of immunotherapy; these agents reconstitute the immune system to target mesothelioma tumor cells by stimulating cell-mediated immune response (78,79). One such agent currently undergoing clinical trials is amatuximab, a monoclonal antibody directed against mesothelin, a glycoprotein over expressed on the cell surface of mesothelioma cells (80). Other agents primarily acting on T-cell activation and function are currently in clinical trials, such as agents targeted to the cytotoxic T-lymphocyte associated antigen 4 (CTLA-4, tremelimumab) and programmed death 1 (PD-1, pembrolizumab, nivolumab) pathways (80). Immunotherapy agents are associated with a variety of immune-related systemic adverse events, such as sarcoid-like mediastinal and hilar lymphadenopathy, dermatitis, thyroiditis, arthritis, myositis, hepatitis, nephritis, enterocolitis, myocarditis and pneumonitis (81).

Conclusions

Tri-modality (surgery, radiotherapy, chemotherapy) therapy in MPM has been associated with improved outcomes in patients with resectable disease (82). There are several complications that have been associated with treatment strategies and can result in significant morbidity; imaging can play a central role in the identification and subsequent management of treatment related complications.

Acknowledgements

None.

Footnote

Conflicts of Interest: The authors have no conflicts of interest to declare.

References

1. Ai J, Stevenson JP. Current issues in malignant pleural mesothelioma evaluation and management. Oncologist 2014;19:975-84.
2. Nickell LT Jr, Lichtenberger JP 3rd, Khorashadi L, et al. Multimodality imaging for characterization, classification, and staging of malignant pleural mesothelioma. Radiographics 2014;34:1692-706.
3. Edwards JG, Abrams KR, Leverment JN, et al. Prognostic factors for malignant mesothelioma in 142 patients: validation of CALGB and EORTC prognostic scoring systems. Thorax 2000;55:731-5.
4. Frauenfelder T, Kestenholz P, Hunziker R, et al. Use of computed tomography and positron emission tomography/computed tomography for staging of local extent in patients with malignant pleural mesothelioma. J Comput Assist Tomogr 2015;39:160-5.
5. Heelan RT, Rusch VW, Begg CB, et al. Staging of malignant pleural mesothelioma: comparison of CT and MR imaging. AJR Am J Roentgenol 1999;172:1039-47.
6. Patz EF Jr, Shaffer K, Piwnica-Worms DR, et al. Malignant pleural mesothelioma: value of CT and MR imaging in predicting resectability. AJR Am J Roentgenol 1992;159:961-6.
7. Gill RR, Umeoka S, Mamata H, et al. Diffusion-weighted MRI of malignant pleural mesothelioma: preliminary assessment of apparent diffusion coefficient in histologic subtypes. AJR Am J Roentgenol 2010;195:W125-30.
8. van Zandwijk N, Clarke C, Henderson D, et al. Guidelines for the diagnosis and treatment of malignant pleural mesothelioma. J Thorac Dis 2013;5:E254-307.
9. Rusch VW. A proposed new international TNM staging system for malignant pleural mesothelioma. From the International Mesothelioma Interest Group. Chest 1995;108:1122-8.

10. Rusch VW, Giroux D. Do we need a revised staging system for malignant pleural mesothelioma? Analysis of the IASLC database. Ann Cardiothorac Surg 2012;1:438-48.
11. Waller DA. The staging of malignant pleural mesothelioma: are we any nearer to squaring the circle? Eur J Cardiothorac Surg 2016;49:1648-9.
12. Taioli E, Wolf AS, Camacho-Rivera M, et al. Determinants of Survival in Malignant Pleural Mesothelioma: A Surveillance, Epidemiology, and End Results (SEER) Study of 14,228 Patients. PLoS One 2015;10:e0145039.
13. Flores RM, Riedel E, Donington JS, et al. Frequency of use and predictors of cancer-directed surgery in the management of malignant pleural mesothelioma in a community-based (Surveillance, Epidemiology, and End Results [SEER]) population. J Thorac Oncol 2010;5:1649-54.
14. Ettinger DS, Wood DE, Akerley W, et al. NCCN Guidelines Insights: Malignant Pleural Mesothelioma, Version 3.2016. J Natl Compr Canc Netw 2016;14:825-36.
15. Rice D, Rusch V, Pass H, et al. Recommendations for uniform definitions of surgical techniques for malignant pleural mesothelioma: a consensus report of the international association for the study of lung cancer international staging committee and the international mesothelioma interest group. J Thorac Oncol 2011;6:1304-12.
16. Wolf AS, Flores RM. Current Treatment of Mesothelioma: Extrapleural Pneumonectomy Versus Pleurectomy/Decortication. Thorac Surg Clin 2016;26:359-75.
17. Taioli E, Wolf AS, Flores RM. Meta-analysis of survival after pleurectomy decortication versus extrapleural pneumonectomy in mesothelioma. Ann Thorac Surg 2015;99:472-80.
18. Flores RM, Pass HI, Seshan VE, et al. Extrapleural pneumonectomy versus pleurectomy/decortication in the surgical management of malignant pleural mesothelioma: results in 663 patients. J Thorac Cardiovasc Surg 2008;135:620-6, 626.e1-3.
19. Opitz I. Management of malignant pleural mesothelioma-The European experience. J Thorac Dis 2014;6:S238-52.
20. Allen KB, Faber LP, Warren WH. Malignant pleural mesothelioma. Extrapleural pneumonectomy and pleurectomy. Chest Surg Clin N Am 1994;4:113-26.
21. Pass HI, Temeck BK, Kranda K, et al. Phase III randomized trial of surgery with or without intraoperative photodynamic therapy and postoperative immunochemotherapy for malignant pleural mesothelioma. Ann Surg Oncol 1997;4:628-33.
22. Pass HI, Kranda K, Temeck BK, et al. Surgically debulked malignant pleural mesothelioma: results and prognostic factors. Ann Surg Oncol 1997;4:215-22.
23. Aziz T, Jilaihawi A, Prakash D. The management of malignant pleural mesothelioma; single centre experience in 10 years. Eur J Cardiothorac Surg 2002;22:298-305.
24. de Vries WJ, Long MA. Treatment of mesothelioma in Bloemfontein, South Africa. Eur J Cardiothorac Surg 2003;24:434-40.
25. Rosenzweig KE, Fox JL, Zelefsky MJ, et al. A pilot trial of high-dose-rate intraoperative radiation therapy for malignant pleural mesothelioma. Brachytherapy 2005;4:30-3.
26. Okada M, Mimura T, Ohbayashi C, et al. Radical surgery for malignant pleural mesothelioma: results and prognosis. Interact Cardiovasc Thorac Surg 2008;7:102-6.
27. Schipper PH, Nichols FC, Thomse KM, et al. Malignant pleural mesothelioma: surgical management in 285 patients. Ann Thorac Surg 2008;85:257-64.
28. Borasio P, Berruti A, Billé A, et al. Malignant pleural mesothelioma: clinicopathologic and survival characteristics in a consecutive series of 394 patients. Eur J Cardiothorac Surg 2008;33:307-13.
29. Mineo TC, Ambrogi V, Cufari ME, et al. May cyclooxygenase-2 (COX-2), p21 and p27 expression affect prognosis and therapeutic strategy of patients with malignant pleural mesothelioma? Eur J Cardiothorac Surg 2010;38:245-52.
30. Luckraz H, Rahman M, Patel N, et al. Three decades of experience in the surgical multi-modality management of pleural mesothelioma. Eur J Cardiothorac Surg 2010;37:552-6.
31. Friedberg JS, Mick R, Culligan M, et al. Photodynamic therapy and the evolution of a lung-sparing surgical treatment for mesothelioma. Ann Thorac Surg 2011;91:1738-45.
32. Rena O, Casadio C. Extrapleural pneumonectomy for early stage malignant pleural mesothelioma: a harmful procedure. Lung Cancer 2012;77:151-5.
33. Nakas A, Waller D, Lau K, et al. The new case for cervical mediastinoscopy in selection for radical surgery for malignant pleural mesothelioma. Eur J Cardiothorac Surg 2012;42:72-6.
34. Nakas A, Meyenfeldt von E, Lau K, et al. Long-term survival after lung-sparing total pleurectomy for locally advanced (International Mesothelioma Interest Group Stage T3-T4) non-sarcomatoid malignant pleural

mesothelioma. Eur J Cardiothorac Surg 2012;41:1031-6.
35. Lang-Lazdunski L, Bille A, Lal R, et al. Pleurectomy/decortication is superior to extrapleural pneumonectomy in the multimodality management of patients with malignant pleural mesothelioma. J Thorac Oncol 2012;7:737-43.
36. Bovolato P, Casadio C, Billè A, et al. Does surgery improve survival of patients with malignant pleural mesothelioma?: a multicenter retrospective analysis of 1365 consecutive patients. J Thorac Oncol 2014;9:390-6.
37. Sugarbaker DJ, Jaklitsch MT, Bueno R, et al. Prevention, early detection, and management of complications after 328 consecutive extrapleural pneumonectomies. J Thorac Cardiovasc Surg 2004;128:138-46.
38. Infante M, Morenghi E, Bottoni E, et al. Comorbidity, postoperative morbidity and survival in patients undergoing radical surgery for malignant pleural mesothelioma. Eur J Cardiothorac Surg 2016;50:1077-82.
39. Welch TD, Ling LH, Espinosa RE, et al. Echocardiographic diagnosis of constrictive pericarditis: Mayo Clinic criteria. Circ Cardiovasc Imaging 2014;7:526-34.
40. Restrepo CS, Lemos DF, Lemos JA, et al. Imaging findings in cardiac tamponade with emphasis on CT. Radiographics 2007;27:1595-610.
41. Restrepo CS, Gutierrez FR, Marmol-Velez JA, et al. Imaging patients with cardiac trauma. Radiographics 2012;32:633-49. Erratum in: Radiographics 2012;32:1258.
42. Tsukada G, Stark P. Postpneumonectomy complications. AJR Am J Roentgenol 1997;169:1363-70.
43. Pool KL, Munden RF, Vaporciyan A, et al. Radiographic imaging features of thoracic complications after pneumonectomy in oncologic patients. Eur J Radiol 2012;81:165-72.
44. Gurney JW, Arnold S, Goodman LR. Impending cardiac herniation: the snow cone sign. Radiology 1986;161:653-5.
45. Wolf AS, Daniel J, Sugarbaker DJ. Surgical techniques for multimodality treatment of malignant pleural mesothelioma: extrapleural pneumonectomy and pleurectomy/decortication. Semin Thorac Cardiovasc Surg 2009;21:132-48.
46. Rotman JA, Plodkowski AJ, Hayes SA, et al. Postoperative complications after thoracic surgery for lung cancer. Clin Imaging 2015;39:735-49.
47. Deslauriers J, Aucoin A, Grégoire J. Postpneumonectomy pulmonary edema. Chest Surg Clin N Am 1998;8:611-31, ix.
48. Billè A, Okiror L, Karenovics W, et al. What is the optimum strategy for thromboembolic prophylaxis following extrapleural pneumonectomy in patients with malignant pleural mesothelioma? Interact Cardiovasc Thorac Surg 2012;15:201-3.
49. ARDS Definition Task Force, Ranieri VM, Rubenfeld GD, et al. Acute respiratory distress syndrome: the Berlin Definition. JAMA 2012;307:2526-33.
50. Zompatori M, Ciccarese F, Fasano L. Overview of current lung imaging in acute respiratory distress syndrome. Eur Respir Rev 2014;23:519-30.
51. Bédard EL, Uy K, Keshavjee S. Postpneumonectomy syndrome: a spectrum of clinical presentations. Ann Thorac Surg 2007;83:1185-8.
52. Wolf AS, Jacobson FL, Tilleman TR, et al. Managing the pneumonectomy space after extrapleural pneumonectomy: postoperative intrathoracic pressure monitoring. Eur J Cardiothorac Surg 2010;37:770-5.
53. McGrath EE, Blades Z, Anderson PB. Chylothorax: aetiology, diagnosis and therapeutic options. Respir Med 2010;104:1-8.
54. Pamarthi V, Stecker MS, Schenker MP, et al. Thoracic duct embolization and disruption for treatment of chylous effusions: experience with 105 patients. J Vasc Interv Radiol 2014;25:1398-404.
55. Pinto PS, Sirlin CB, Andrade-Barreto OA, et al. Cisterna chyli at routine abdominal MR imaging: a normal anatomic structure in the retrocrural space. Radiographics 2004;24:809-17.
56. Massard G, Ducrocq X, Hentz JG, et al. Esophagopleural fistula: an early and long-term complication after pneumonectomy. Ann Thorac Surg 1994;58:1437-40; discussion 1441.
57. Noh D, Park CK. The Management of Delayed Post-Pneumonectomy Broncho-Pleural Fistula and Esophago-Pleural Fistula. Korean J Thorac Cardiovasc Surg 2016;49:138-40.
58. Ohri N, Taioli E, Ehsani M, et al. Definitive Radiation Therapy Is Associated With Improved Survival in Non-Metastatic Malignant Pleural Mesothelioma. Int J Radiat Oncol Biol Phys 2016;96:S132-3.
59. Thieke C, Nicolay NH, Sterzing F, et al. Long-term results in malignant pleural mesothelioma treated with neoadjuvant chemotherapy, extrapleural pneumonectomy and intensity-modulated radiotherapy. Radiat Oncol 2015;10:267.
60. Cho BC, Feld R, Leighl N, et al. A feasibility study evaluating Surgery for Mesothelioma After Radiation Therapy: the "SMART" approach for resectable malignant pleural mesothelioma. J Thorac Oncol 2014;9:397-402.
61. Mordant P, McRae K, Cho J, et al. Impact of induction

therapy on postoperative outcome after extrapleural pneumonectomy for malignant pleural mesothelioma: does induction-accelerated hemithoracic radiation increase the surgical risk? Eur J Cardiothorac Surg 2016;50:433-8.
62. Allen AM, Czerminska M, Jänne PA, et al. Fatal pneumonitis associated with intensity-modulated radiation therapy for mesothelioma. Int J Radiat Oncol Biol Phys 2006;65:640-5.
63. Larici AR, del Ciello A, Maggi F, et al. Lung abnormalities at multimodality imaging after radiation therapy for non-small cell lung cancer. Radiographics 2011;31:771-89.
64. Rosenzweig KE. Current readings: improvements in intensity-modulated radiation therapy for malignant pleural mesothelioma. Semin Thorac Cardiovasc Surg 2013;25:245-50.
65. Rimner A, Zauderer MG, Gomez DR, et al. Phase II Study of Hemithoracic Intensity-Modulated Pleural Radiation Therapy (IMPRINT) As Part of Lung-Sparing Multimodality Therapy in Patients With Malignant Pleural Mesothelioma. J Clin Oncol 2016;34:2761-8.
66. Ideguchi H, Kojima K, Hirosako S, et al. Cisplatin-induced eosinophilic pneumonia. Case Rep Pulmonol 2014;2014:209732.
67. Breuer S, Nechushtan H. Pemetrexed-induced lung toxicity: a case report. Clin Oncol (R Coll Radiol) 2012;24:76-7.
68. Dhakal B, Singh V, Shrestha A, et al. Pemetrexed induced pneumonitis. Clin Pract 2011;1:e106.
69. Kurimoto R, Sekine I, Iwasawa S, et al. Alveolar hemorrhage associated with pemetrexed administration. Intern Med 2015;54:833-6.
70. Kato M, Shukuya T, Takahashi F, et al. Pemetrexed for advanced non-small cell lung cancer patients with interstitial lung disease. BMC Cancer 2014;14:508.
71. Nagata K, Kaji R, Tomii K. Fatal pemetrexed-induced lung injury in patients with advanced mesothelioma: a report of two cases. J Thorac Oncol 2010;5:1714-5.
72. Belknap SM, Kuzel TM, Yarnold PR, et al. Clinical features and correlates of gemcitabine-associated lung injury: findings from the RADAR project. Cancer 2006;106:2051-7.
73. Sugarbaker DJ, Gill RR, Yeap BY, et al. Hyperthermic intraoperative pleural cisplatin chemotherapy extends interval to recurrence and survival among low-risk patients with malignant pleural mesothelioma undergoing surgical macroscopic complete resection. J Thorac Cardiovasc Surg 2013;145:955-63.
74. Tilleman TR, Richards WG, Zellos L, et al. Extrapleural pneumonectomy followed by intracavitary intraoperative hyperthermic cisplatin with pharmacologic cytoprotection for treatment of malignant pleural mesothelioma: a phase II prospective study. J Thorac Cardiovasc Surg 2009;138:405-11.
75. Friedberg JS, Simone CB 2nd, Culligan MJ, et al. Extended Pleurectomy-Decortication-Based Treatment for Advanced Stage Epithelial Mesothelioma Yielding a Median Survival of Nearly Three Years. Ann Thorac Surg 2017;103:912-9.
76. Nishino M, Hatabu H, Johnson BE, et al. State of the art: Response assessment in lung cancer in the era of genomic medicine. Radiology 2014;271:6-27.
77. Ferretti GR, Reymond E, Delouche A, et al. Personalized chemotherapy of lung cancer: What the radiologist should know. Diagn Interv Imaging 2016;97:287-96.
78. Bograd AJ, Suzuki K, Vertes E, et al. Immune responses and immunotherapeutic interventions in malignant pleural mesothelioma. Cancer Immunol Immunother 2011;60:1509-27.
79. Wong RM, Ianculescu I, Sharma S, et al. Immunotherapy for malignant pleural mesothelioma. Current status and future prospects. Am J Respir Cell Mol Biol 2014;50:870-5.
80. Bonelli MA, Fumarola C, La Monica S, et al. New therapeutic strategies for malignant pleural mesothelioma. Biochem Pharmacol 2017;123:8-18.
81. Nishino M, Tirumani SH, Ramaiya NH, et al. Cancer immunotherapy and immune-related response assessment: The role of radiologists in the new arena of cancer treatment. Eur J Radiol 2015;84:1259-68.
82. Wald O, Sugarbaker DJ. Perspective on malignant pleural mesothelioma diagnosis and treatment. Ann Transl Med 2016;4:120.

Cite this article as: Murphy DJ, Gill RR. Overview of treatment related complications in malignant pleural mesothelioma. Ann Transl Med 2017;5(11):235. doi: 10.21037/atm.2017.03.97

